VIBRATION ANALYSIS OF THE ISIS SYNCHROTRON DIPOLE MAGNETS

J. Brower, A. Yaqoob, Rutherford Appleton Laboratory, Oxfordshire, UK
G. Squicciarini, N. S. Ferguson, ISVR University of Southampton, Hampshire, UK

1.   Abstract

The ISIS synchrotron uses dipole magnets to steer the proton beam to maintain a fixed radius circular orbit. The beam energy is synchronised to the 50 Hz magnetic field as protons accelerate from 70 to 800 MeV before extraction. The failure of a single dipole causes several days of costly machine downtime. ISIS currently employs a simple form of manual vibration monitoring to assess magnet health before each machine cycle.

In this paper we discuss a new condition monitoring scheme that utilises modern technology, to perform remote vibration monitoring and analysis in real time during beam operation. Two dipole magnets were instrumented and data were acquired across two adjacent cycles of operation. The results show the quality of data achievable from this hostile environment. Data analysis, using proven experimental methods, characterised the magnets and plotted performance over time as a proof of concept prior to a full rollout of the system.
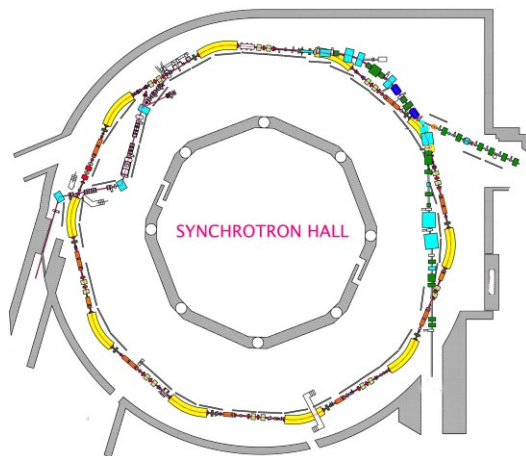
2.   Introduction

Figure 1 – The ISIS synchrotron with its ten operational dipole magnets highlighted in yellow

ISIS, located at the Rutherford Appleton Laboratory, is a world-class pulsed spallation neutron source providing neutrons and muons to scientists probing the microscopic structure and dynamics of matter. The facility operates 24/7 during user cycles of 4–6 weeks for a total of up to 180 days a year. Neutron production begins with the ion source which produces H- ions that accelerate to 70 MeV within the linear accelerator. After charge-exchange injection, the protons in the synchrotron are accelerated further to 800 MeV before extraction to two target stations. Spalled neutrons from two tantalum-clad tungsten targets are directed to an array of experimental beamlines, each designed for particular experimental techniques.

Figure 2 – Synchrotron dipole magnet

The synchrotron contains ten super-periods (SP), each accommodating one 30 tonne dipole magnet (identified as D0-9) (Fig.2). Each dipole comprises an upper and lower yoke supporting an upper and lower coil, which collectively surround the vacuum vessel. A 3 MW main magnet power supply (MMPS) delivers up to 400 A AC at 50 Hz superimposed on a 662 A DC current. This generates a ramping 0.2 - 0.7 T magnetic field, bending the beam 36 degrees laterally in each straight.

Since 1985, 32 unexpected dipole failures have occurred costing several weeks' downtime [1] primarily from coil arcs causing water leaks in the coil capillaries.   The root cause may originate from electrical systems and the coils themselves; i.e. their type and ageing properties [2]. In an attempt to mitigate failures, technicians use a three metre probe connected to a Pruftechnik VIBXpert device to record vibration at specific points on the magnets. The assumption is that abnormal magnet operation will manifest itself through changes in the vibration signatures. This method has many weaknesses: lack of continuity in recorded data as measurement points are not precisely repeatable, data chronicling failure events during operation are not captured and entry into the synchrotron has safety risks primarily from radiation doses and electrical safety to personnel.

3.   Methodology

A radiation survey [4] identified D6 and D7 to be relatively inactive (typically 16 µSV/h at the upstream yoke face and 5 µSV/h at the top). Finite element analysis on a dipole model using Vector Fields Opera

[3] predicted flux densities of <10 mT could be achieved by strategically placing sensors on magnet coil brackets. The accelerometers chosen were radiation hardened charge-output devices (PCB Piezotronics model 357B53) with piezo ceramic elements generating 100 pC/g. 15 m of low noise coaxial cable (PCB Piezotronics 003A) housed in earthed KOPEX trunking fed conditioning amplifiers (PCB Piezotronics 422E03) generating 100 mV/g.

Figure 3 – Termination boxes housing in-line conditioning amplifiers and wiring beneath synchrotron hall floor

The amplifiers were placed in screened boxes within cable ducting (Fig 3) from which 20 m of coaxial cable connected them to National Instruments® (NI) [6] data acquisition (DAQ) equipment housed in a low activity shielded area. In total, eight removable sensors were held by screw threads using PEEK washers glued to equipment. These were attached to the yokes, coil brackets and vacuum vessel of D6 and D7 (Fig 4). Three further sensors were used: one dummy sensor to quantify induced environment cable noise, one floor mounted sensor to quantify room vibration and one sensor with no earthed trunking to further compare induced cable noise. The DAQ system employed was a PXI chassis containing a PXIe-6133 controller and PXIe-4497 sound and vibration module. The module delivered a 4 mA current excitation powering the amplifiers, with anti-aliasing filters providing additional signal conditioning.
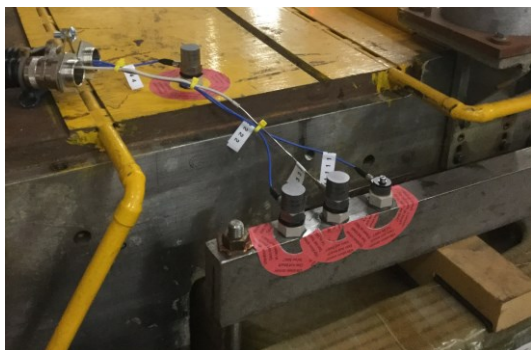

Figure 4 – Sensors on upstream yoke and coil bracket of D7

All eight channels were AC-coupled and pre-calibrated to ensure measurement accuracy. A LabVIEW VI was constructed to log the accelerometer data, containing separate analysis loops for analysing acceleration amplitude, RMS, FFT and kurtosis. The Nyquist criterion was satisfied by using a 3 kHz sample rate, minimising aliasing across the band up to 1 kHz. All data were logged in TDMS files and MMPS [5] AC and DC operational data were logged for correlation. Additionally, an instrumented hammer impact test was carried out on the D7 yoke to characterise the intrinsic structural modes.

4. Results

The study collected 1.5 TB of data across 90 days of operation from 11 sensor locations. The typical signal-to-noise ratio (S/N) of the data was >20 dB from all sensors. Comparing data from two adjacent sensors (s/n 47639 & s/n 47640) mounted on the downstream upper yoke following the same cabling route, one using earthed KOPEX trunking and one without, showed no difference to the S/N ratio. Comparisons between the dummy sensor (s/n 47210) and an adjacent sensor (s/n 47208) mounted on the upstream coil bracket of D7 again showed no impact on signal quality from extraneous noise at full beam energy. Sensors mounted adjacent to magnetic field of <80 mG on the coil bracket of D7 had no measurable interference. There was also no measureable impact on any data within the measured bandwidth from any sensor due to RF, radiation or beam however there was 50 Hz electrical noise in the recorded data (Fig 8)
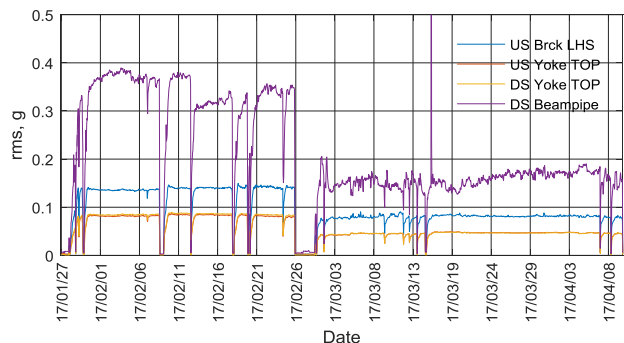

Figure 5 - RMS vibration levels for D7 during first cycle of machine operation

Figure 5 shows the acceleration data from sensors on both ends of the yoke, coil bracket and down-stream vacuum vessel (beampipe) of D7. The time window of the RMS measurements was 3 minutes but if reduced, would clearly show more frequent events due to increased granularity. Sudden drops in vibration occurred at various times due to MMPS rundown, temporary faults or planned shut-down maintenance. The vibration levels of the vacuum vessel were the highest at 0.3-0.4 g across the duration of February, peaking on February 4th. This component showed the biggest fluctuation over time and took the longest to reach a steady-state amplitude after a shut-down period. All four traces show a significant drop in vibration levels on 26th February when the beam energy was intentionally reduced to 700 MeV after the

maintenance day. The sharp peak occurring on the 14th March is unclear, possibly due to a momentary sensor or acquisition fault.
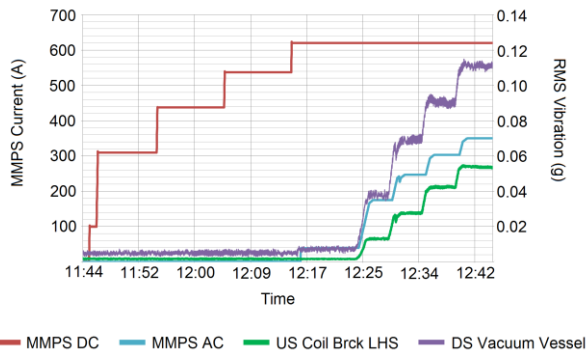

Figure 6 - Correlation between MMPS current ramp and D7 vibration

Figure 6 shows a more detailed view of the MMPS DC and AC outputs together with the corresponding RMS vibration from two sensors on D7; the upstream coil bracket (s/n 47208) and vacuum vessel (s/n 47641). The AC ramping is clearly identifiable from the sensors showing that the vacuum vessel has double the amplitude, this is as yet unexplained. For all of the acquired data, the frequency content of the vibration exhibits discrete tonal components at multiple integers of 50 Hz with the 100 Hz component dominant (Fig 7). This was found to be 10-20 dB above the 50 Hz component. Higher order harmonics were also clearly evident in the spectrum up to the maximum frequency analysed, but these were generally at least 20 dB below the 100 Hz component. In addition to the 50 Hz harmonics, there was also a series of harmonics for a fundamental frequency component of 25 Hz, these were much lower in level (60-80 dB below the 100 Hz) and may reflect the presence of a vibration mode at nearly 25 Hz.

To confirm that the data from D7 was representative, measurements were taken over 10 days of a second cycle of operation from identical downstream yokes located on D6 and D7 (s/n 47640 and s/n 47639). Figure 7 upper graph shows similar amplitudes of 0.2 g peak to peak with a small phase difference and the lower graph, using FFT analysis, shows identical frequency components, however with different amplitudes.

To identify how different magnet components vibrate with respect to each other, modal analysis on the response data was conducted using controlled excitation to identify the natural frequencies, mode shapes and damping. Figure 8 shows the transfer functions between the acceleration responses measured at the upstream yoke sensor (s/n 47211) and the force from an impact hammer. The latter was applied at four points on the top of the yoke, p1 to p4, which were equally spaced on the top of the yoke between the upstream end and the magnet longitudinal midpoint respectively. There was a clear presence of a vibration mode at around 26Hz with all four points moving in phase. There were peaks at 40 and 50 Hz; the latter was likely due to electrical noise while the reason for the 40 Hz remains unclear.
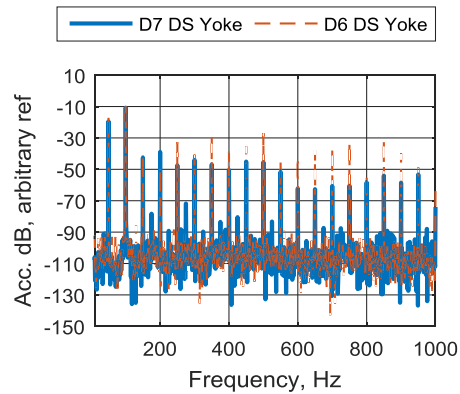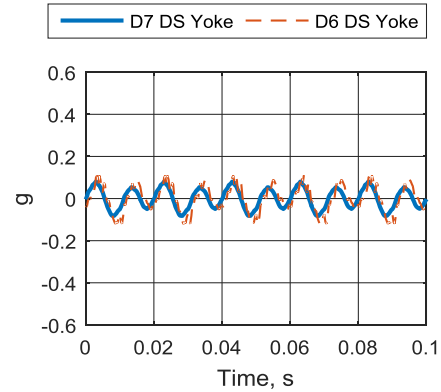

Figure 7 - Data from downstream yoke on D6 and D7. Upper graph time domain signals and lower graph corresponding frequency spectra

Neither of these two peaks showed the 180° change of phase typical of vibration modes as they pass through resonance and the coherence function (not shown here) drops in this range. At around 93 Hz there is a broad peak and at the same frequency the phase for points p1 to p3 shows the 180° change of phase.
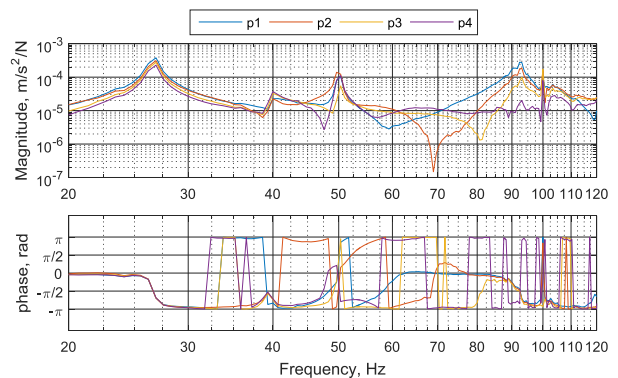

Figure 8 - Magnitude and phase of measured point and transfer accelerances at 4 points on the top of the yoke of D7 for excitation at point p1
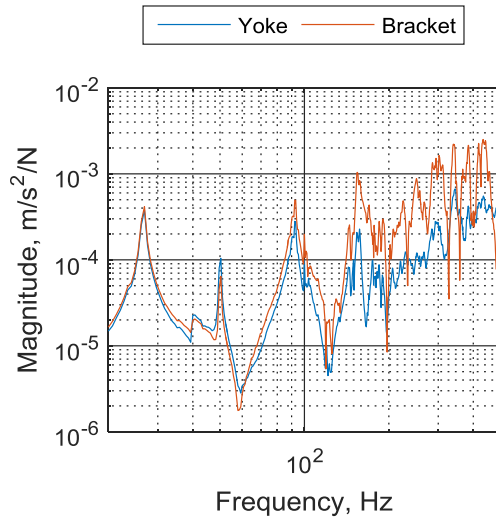
Figure 9 - Point accelerances measured on the yoke of D7 at p1 and transfer accelerance between p1 and the coil bracket

Figure 9 shows the point accelerance at p1 compared with the transfer accelerance between p1 and the sensor on the coil bracket (s/n 47208). Two natural frequencies were identified at 26.7 Hz and 92.3 Hz. The damping ratio was 11.3% for mode 1 and 15% for mode 2. The yoke and the coil bracket were found to vibrate with the same amplitude and phase (not shown here) up to 100 Hz, above which the higher flexibility of the bracket resulted in higher vibration levels and different phases.

5. Discussion

Catastrophic faults which can occur within milliseconds may have associated long-term vibrational trends visible, at least qualitatively, in the time and frequency domain. This warrants the need to store data for at least a cycle to analyse and learn from the behaviour. Different vibration amplitudes, frequencies and phases have been measured between different system components, some less tightly mechanically coupled, especially at high modes. Such components may indicate forthcoming failures with greater accuracy e.g. coils over yokes, which reinforces the need to sensor them separately.

It is reasonable to predict that information above a given frequency, say 300 Hz, would add diminished value to condition monitoring. This would result in a big reduction in data overhead as compared to this study (3 kHz sampling rate). It is possible that 100 Hz is the dominant frequency since there is a vibration mode close-by at 93 Hz. Whilst 93 Hz is not exactly the second harmonic of the magnetic field (100 Hz) it is close enough to be amplified with respect to 50 Hz. It is also possible that the magnetic field has important components at higher harmonics of the 50 Hz due to saturation and subsequent non-linearity. It is not clear why the two sides of the yoke vibrate in phase at 100 Hz (data not shown in paper) while there is a vibration mode at 93Hz with the two sides vibrating in opposite phase. It is possible that

the different nature of the forcing is resulting in different behaviour during the operational condition. The instrumented impact hammer used during the modal analysis tests was applied at single points, whilst the magnetic field and associated forcing is distributed over the entire length of the dipole. In the ideal case of a distributed force over the magnet yoke the second mode should not be excited because the modal component of the force cancels over the length. It is possible that the magnet fringe fields result in some excitation of the second mode, but this does not fully explain why the two sides are in phase during the cycle and out of phase in the modal analysis tests. It is also not clear why the beam pipe has an unexpected phase difference (140°) with respect to the yoke.

6. Conclusion

The aspiration to implement a remote vibration condition monitoring system in the synchrotron at ISIS was bounded by a number of technical issues that this study aimed to clarify. Firstly, robust and reliable vibrational data needed to be extracted from the hostile environment. 1.5 TB of raw data was successfully collected from D6 and D7 for real-time monitoring and stored for later analysis. By using charge mode accelerometers, low noise cable and electronic equipment shielded from thermal neutrons, the systems were unaffected by high B-fields, radiation and RF interference. The S/N ratio was >20 dB and there was no advantage gained by using shielded trunking for the low noise coaxial cable other than protection from cable damage.

The study aimed to see if operational events concerning the dipoles manifest themselves in vibrational data so the system could be used to analyse trends and predict failure. Data was of sufficient quality to see operational events in some detail ranging from machine dropouts, energy changes, ramping start-up and shutdown but no faults occurred to allow analysis surrounding a specific dipole failure. Data revealed detailed RMS and frequency information sufficient to characterise magnets and learn how they behave. Modal analysis showed dominant vibrational modes and clarified the need to individually sensor yokes, coil brackets and vacuum vessels. Trend analysis was also found to be feasible over longer timescales and FFT analysis showed harmonic components extending up to 1 kHz.

By comparing data from sensors across the system, the study was able to learn the relationship between different components, specifically between the vacuum vessel and adjacent yoke and coil. There was an immediate benefit to ISIS in having quality real-time vibrational data available remotely outside the synchrotron. By replacing the manual testing routine for D6 and D7 in this study, personnel were not exposed to radiation or electrical safety risks. The stored data allowed analysis of magnet operations over two cycles so individual events could be inspected for diagnostic purposes. The study achieved its objectives to prove that vibrational data from dipole magnets was

accessible, collectable and useful in understanding the systems. While continued testing is needed to capture a component failure and demonstrate that such events may be predictable, there is sufficient confidence from this study to roll out a condition monitoring system across the whole of the ISIS synchrotron.

References

[1] S Kellard, "Dipole Failure Analysis", ISIS Accelerator Design Group, June 2017

[2] S Kellard, " Synchrotron Dipole Failure Analysis – Update", ISIS Accelerator Design Group, Nov. 2014

[3] M Hughes, "ISIS Dipole vibration sensor placement study", ISIS Electrical Engineering Group, Sept. 2016

[4] Dipole surveys in synchrotron John Moir Health Physics 11/08/2016 and STFC ISIS Health Physics Survey Dipole 7 John Moir 04/01/2107

[5] Contributed by J. Ranner, ISIS Electrical Engineering Department

[6] National Instruments and LabVIEW are registered trademarks of the National Instruments Corporation.